Building Energy Models with Morphological Urban-Scale Parameters: A Case Study in Turin

Roberto Boghetti – University of Pisa, Italy – roberto.boghetti@studenti.unipi.it
Fabio Fantozzi – University of Pisa, Italy – fabio.fantozzi@unipi.it
Jérôme Kämpf – Idiap Research Institute, Switzerland – jerome.kaempf@idiap.ch
Guglielmina Mutani – Politecnico di Torino, Italy – guglielmina.mutani@polito.it
Giacomo Salvadori – University of Pisa, Italy – giacomo.salvadori@unipi.it
Valeria Todeschi – Politecnico di Torino, Italy – valeria.todeschi@polito.it

Abstract

With a growing awareness around the importance of the optimization of building efficiency, being able to make accurate predictions of building energy demand is an invaluable asset for practitioners and designers. For this reason, it is important to continually improve existing models as well as introduce new methods that can help reduce the so-called energy performance gap, which separates predicted from actual consumption values. This is particularly true for urban scale simulations, where even small scenes can be very complex and carry the necessity of finding a reasonable balance between precision and computational efforts. The scope of this work is to present two different models that make use of morphological urban-scale parameters to improve their performances, taking into account the interactions between buildings and their surroundings. In order to do this, two neighbourhoods in the city of Turin (IT) were taken as case studies. The buildings studied present similar characteristics but are inserted in a different urban context. Several urban parameters were extracted using a GIS tool and used as input, alongside the building-scale features, for two different models: i) a bottom-up engineering approach that evaluates the energy balance of residential buildings and introduces some variables at block-of-buildings scale, ii) a machine learning approach based on the bootstrap aggregating (bagging) algorithm, which takes the same parameters used by the previous model as inputs and makes an estimation of the hourly energy consumption of each building. The main results obtained confirm that the urban context strongly influences the energy performance of buildings located in high built-up areas, and that introducing simple morphological urban-scale parameters in the models to take these effects into account can improve their performance while having a very low impact on the computational efforts.

1. Introduction

One of the key challenges of our century is to alleviate human pressure on the environment and particularly to slow down the climate change that greenhouse gas emissions are accelerating (Verbeke and Audenaert, 2018). The buildings sector accounts for a large share of the total energy-related CO_2 emissions - around 28% in 2018 - and it will therefore play a central role in the clean energy transition (IEA, 2019). In particular, the reduction of energy consumption in buildings, together with the transition to renewable energies, could be one of the main drivers of this turnaround (Mutani and Todeschi, 2018). An important step to achieve this goal is to develop robust models that allow us to make reliable estimates of the energy demand of buildings, which can be used as a base for planning the city of tomorrow (Streicher et al., 2019). However, building these models at urban scale is a complex task, as the energy consumption depends on several factors at different scales, such as the dynamic interaction between the outdoor climate and the specific characteristics of the building's surroundings, the thermal characteristics of its envelope elements and technical systems (Caruso et al., 2013; Palme et al., 2017; Perera et al., 2018).

In this work, two energy models for residential buildings that take into account morphological urban-scale parameters are presented, evaluated and discussed. Comparable studies include (Hedegaard et al., 2019; Mutani and Todeschi, 2019; Nageler et al., 2017; Sola et al., 2018) for energy models and (Amasyali and El-Gohary, 2018; Boghetti et al., 2019) for data-driven ones.

2. Materials and Methods

This section describes two different approaches to create building energy models at neighborhood scale. The first is a bottom-up engineering model (hourly thermal balance), while the second one is a data-driven model based on the Bagging algorithm. Fig. 1 indicates the input data and the procedure used to compare the models.

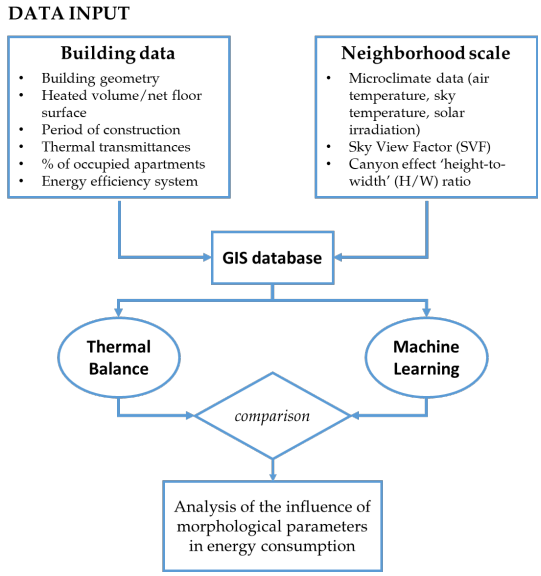

Fig. 1 – Flowchart of energy models comparison

2.1 Bottom-Up Engineering Model

Starting from previous research (Mutani et al., 2019), a bottom-up engineering hourly energy balance model for residential buildings was created. To evaluate the energy balance of buildings in a built-up urban context, the ISO 52016-1:2017 and ISO 52017-1:2017 standards were used, and the equations were implemented to consider only the data available at neighborhood scale and some morphological urban-scale parameters. The urban parameters used to create the model and to evaluate how the urban form affects the thermal energy consumption in buildings were: the canyon effect, which was quantified using the 'height-to-width' (H/W) ratio, this parameter is able to describe the typical urban microclimate around the buildings; the obstructions, the solar exposition and the thermal were evaluated with the H/W ratio and the Sky View Factor (SVF), which measures the visible portion of the sky from a given location (Middela et al., 2018); the climate and microclimate conditions were downloaded from the nearest weather station.

This section presents an engineering method based on energy balances with hourly time step by considering the main components of a building: the envelope, the glazing and the inside part of a building with the internal structures, the furniture and the air. An iterative procedure makes it possible to calculate the hourly temperatures of the three thermodynamic systems (Fig. 2). In this work, the following assumptions were adopted:

- the temperatures of the thermodynamic systems are uniform;
- heat conduction through the buildings elements is one-dimensional;
- thermal bridges are neglected;
- latent components of influx or out flux of moisture and the heat flow rates for humidification and dehumidification were neglected.

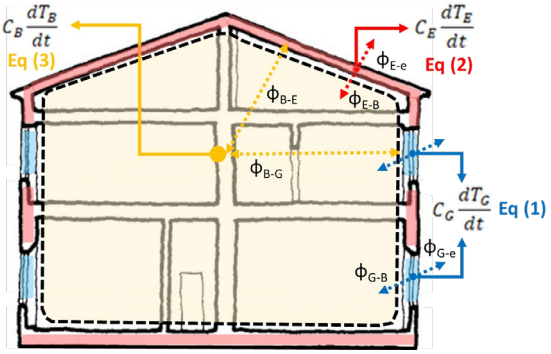

Fig. 2 – The three thermodynamic systems of the engineering dynamic model: B = internal structures, furniture and air; E = opaque envelope; G = glass

2.1.1 Thermal balance of the glasses

The hourly temperature of the glasses (G) of a building were obtained with the balance of the thermal flows between the glasses and the building (B) and the glasses and the outdoor environment (e) (Eq. 1).

$$C_G \frac{dT_G}{dt} = \sum \alpha_G \cdot I \cdot F \cdot A_G - \sum \frac{A_G}{\frac{1}{2} \cdot R_G + R_{se}} \cdot \cdot (T_G - T_{ae}) - \sum \frac{A_G}{\frac{1}{2} \cdot R_G + R_{si}} \cdot (T_G - T_B) - \emptyset_r \quad (1)$$

The term on the left side of Equation 1 describes how the energy stored in windows glasses changes with the time. The terms on the right side of the equation describe the absorption of solar irradiance

(I) and the heat fluxes for transmission between the glasses and the building and between the glasses and the external environment. For every hour, a coefficient is calculated to define the percentage of sunny surfaces as a function of the height of the sun and of the urban canyon height to distance ratio H/W (Mutani et al., 2019). The remaining terms, listed below, refer to:

- the heat flows by transmission between the glasses and the external environment:

$$\sum \frac{A_G}{\frac{1}{2} \cdot R_G + R_{se}} \cdot (T_G - T_{ae})$$

- the heat flows by transmission between the glasses and the internal building quota:

- $$\sum \frac{A_G}{\frac{1}{2} \cdot R_G + R_{si}} \cdot (T_G - T_B)$$

The thermal capacity of the glasses C_G was calculated by considering the specific heat and the mass of the glasses.

2.1.2 Thermal balance of the envelope

The thermal balance of the heat flows for the building envelope was calculated using Equation 2.

$$C_E \frac{dT_E}{dt} = \sum \alpha_E \cdot I \cdot F \cdot A_E - \sum \frac{A_E}{\frac{1}{2} \cdot R_E + R_{se}} \cdot$$

$$\cdot (T_E - T_{ae}) - \sum \frac{A_E}{\frac{1}{2} \cdot R_E + R_{si}} \cdot (T_E - T_B) - \emptyset_r \quad (2)$$

Similarly to Equation 1, the term on the left side describes how the energy stored in the envelope changes with the time; the terms on the left side describe the absorption of solar irradiance, the heat flow by transmission to the building and the external environment and the extra heat flow Φ_r due to thermal radiation to the sky from the envelope. The Φ_r depends on the shading reduction factor for the external obstructions F_{sh} and it was calculated with the SVF (Mutani et al., 2019; Mutani and Todeschi, under revision).

2.1.3 Thermal balance of the building

The thermal balance of the heat flows of the internal building components was calculated using Equation 3:

$$C_B \frac{dT_B}{dt} = \emptyset_H + \emptyset_I + \sum \tau_G \cdot I \cdot F \cdot A_G - \sum \frac{A_E}{\frac{1}{2} \cdot R_E + R_{si}} \cdot (T_B - T_E) -$$

$$- \sum \frac{A_G}{\frac{1}{2} \cdot R_G + R_{si}} \cdot (T_B - T_G) - c_a \cdot \dot{m}_a \cdot (T_{B,ai} - T_{ae}) \quad (3)$$

The term on the left side of the Equation 3 describes how the energy stored inside the building changes with the time. On the right side, the first two terms i) Φ_H and ii) Φ_I described respectively i) the heat flow released by the heating system, which can be calculated by multiplying the energy supplied to the heating system for the system efficiency η_H (Mutani and Todeschi, under review) and ii) the heat flow rate due to internal heat sources that, for residential buildings, depends on the useful heated floor area and the average floor area per dwelling. The third term describes the solar transmission through the transparent elements with the F reduction factor calculated likewise in Equations 1 and 2. The last terms describe the heat flow rates by transmission and ventilation. For the internal heat gains and heat flow for ventilation, the hourly profiles that characterize the users' behavior in the Italian Standard UNI/TS 11300-1:2014 were utilized.

2.2 Bagging Model

The second model uses a machine learning approach based on the bootstrap aggregating (bagging) algorithm (Breiman, 1996) applied to a decision tree regressor. This method was chosen over other possible regression techniques as it provided better and more consistent results on the available data. The bagging algorithm works by sampling the data with replacement, running the prediction method(s) on the samples and finally aggregating the results by averaging the outputs. The decision tree regressor, on the other hand, is a simple learning algorithm that creates a set of binary rules to calculate the target value. The model was trained using real hourly consumption data from buildings of the two neighbourhoods that are not in the input database. As the output of a similar model is dependent on the decision trees that are generated for the bagging algorithm, the results given in this paper are averaged over the outputs of different instances of the model.

2.2.1 Model creation

The model was created using Scikit-learn (Pedregosa et al., 2011) and follows a standard workflow for machine learning applications. In the first phase, the data from the full database was pre-processed. Cat-

egorical features were converted into numerical data and the values of the whole database were scaled. While scaling is not necessary when using the decision tree regressor, it allows for efficient comparison of the results with those of other algorithms within the same script. The evaluated sample is then split from the training set as explained in Section 3.2. Once the data was processed, a first model was created and its performance evaluated. At this point, a backward feature elimination was performed in order to reduce the number of variables by eliminating those that were negatively affecting the performances of the algorithm. This dimensionality reduction method works by excluding one feature at a time and evaluating how the removal affects the performance of the model. If the precision improves, the feature is removed. The process continues iteratively until no variable can be dropped without a negative effect on the performances of the model. Morphological urban-scale parameters were not included in this step as the evaluation of their importance will be carried out subsequently. At the end of this process the resulting model was finally evaluated, and as an acceptable level of precision was reached no further improvements were made.

3. Case Study

Turin is located in the north-western part of Italy, in a continental temperate climate. In Turin there are about 60,000 heated buildings, nearly 45,000 of which are residential. These are mainly large and compact condominiums, and 80% of them were built before 1970 (Amasyali and El-Gohary, 2018; Hedegaard et al., 2019; Middela et al., 2018). In order to evaluate the influence of urban morphology on the consumption of buildings, two neighbourhoods –with similar building characteristics but different urban contexts– are taken as case studies. In the *Einaudi* (E) neighbourhood the buildings have a H/W average value of 0.56 and SVF of 0.63; while in the *Sacchi* (S) area these urban parameters have higher values, 0.64 and 0.76, respectively (Fig.s 3 and 4).

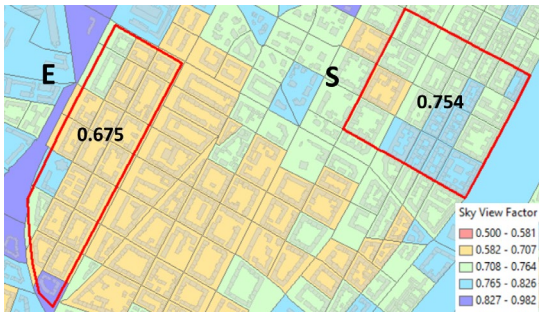

Fig. 3 – Sky View Factor (SVF) calculated with the use of GIS tool, Relief Visualization Toolbox, and the DSM

Fig. 4 – The canyon effect H/W calculated with the use of building characteristics at census section scale

3.1 Data Collection

The urban scale data as well as the geographic information were elaborated with the support of a Geographic Information System (GIS) tool, and a georeferenced database was created using the data presented below:

- *Building data* elaborated using: the Municipal Technical Map[1]; the Territorial Database of the Region[2]; and the socio-economic data (ISTAT census database[3]).
- *Microclimate data* elaborated using *Politecnico* weather station measurements (heating degree days, air temperature, relative humidity, direct solar radiation).
- *Morphological urban-scale parameters* elaborated using *building data*, Satellite Images (Landsat 7 and 8) with a precision of 30 meters available from the USGS website; and the Digital Surface Model (DSM) of Turin with a precision of 5 meters provided by Piedmont Region.
- *Energy consumption data* were provided by the district heating IREN Company of Turin. The

1 http://geoportale.comune.torino.it/web/
2 http://www.geoportale.piemonte.it/cms/
3 http://datiopen.istat.it/

hourly space heating energy consumption refer to the season 2014-15.

3.2 Sampling

Among the available data, a representative sample of buildings was chosen as case study and used as a testing set for both models. The main reasons for using only a subset of the whole database were to save enough buildings to train the machine learning model and to reduce the high computational times of the bottom-up approach. The sampling was carried out on a random basis. Outliers, however, were excluded from the population beforehand in order to avoid errors correlated with the lack of variety in the training data, which would not have been meaningful for the evaluation of morphological urban-scale parameters. Fig.s 5 and 6 show the distribution of the values for the SVF and H/W ratio of the sample compared with those of the full database.

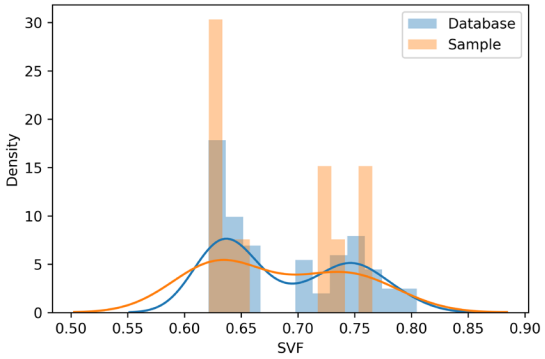

Fig. 5 – Distribution of the Sky View Factor values within the full database (in blue) and the sample (in orange)

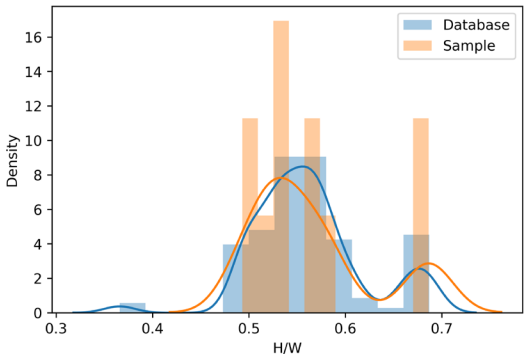

Fig. 6 – Distribution of the Canyon Effect (H/W) values within the full database (in blue) and the sample (in orange)

An overview of the distribution of these parameters in the sample can be found in Table 1, along with the period of construction, the S/V ratio and the thermal transmittances of the buildings.

Table 1 – Characteristics of a selected buildings in the *Einaudi* and *Sacchi* neighborhoods

IDbz	Period	S/V	U_E	U_G	U_g	U_r	H/W	SVF
E-129	19 - 45	0.280	1.35	4.75	0.79	1.76	0.589	0.627
E-132	46 - 60	0.290	1.18	4.4	0.615	1.35	0.569	0.621
E-187	46 - 60	0.286	1.18	4.4	0.615	1.35	0.522	0.650
E-202	61 - 70	0.285	1.13	4.9	0.65	1.49	0.569	0.621
E-227	61 - 70	0.413	1.13	4.9	0.65	1.49	0.589	0.627
S-46	19 - 45	0.344	1.35	4.75	0.79	1.76	0.533	0.722
S-202	19 - 45	0.336	1.35	4.75	0.79	1.76	0.675	0.747
S-262	19 - 45	0.346	1.35	4.75	0.79	1.76	0.600	0.782
S-268	46 - 60	0.404	1.18	4.4	0.615	1.35	0.686	0.765
S-97	61 - 70	0.323	1.13	4.9	0.65	1.49	0.686	0.765

4. Results and Discussion

In this section, the performances of the two models are compared and discussed, along with the improvements that urban parameters have brought in each case. From this work it emerges that urban parameters have a positive impact on the precision of both tested models: the solar exposure and heat exchanges with the external environment significantly influence energy consumption. In particular, in favourable conditions, with high values of SVF and good orientation, energy consumption is lower than in unfavourable conditions (low values of SVF and orientation). Moreover, the shape of the building is fundamental in its heat exchange, and the canyon effect H/W was used to describe the built environment compactness and the type of the surrounding open spaces. In terms of the two models, the following sections detail the results. In general, using a machine learning approach leads to better performances in terms of time and precision. On the other hand, its reliance on the availability of a comprehensive dataset for the training phase makes it less flexible and undermines its performances on heavily heterogeneous case studies.

4.1 Bottom-Up Engineering Model

This section reports the results obtained from the application of the hourly thermal balance model. To present the results, some buildings were selected based on the period of construction, the characteristics of urban context and the type of adjacent street, the consumption of buildings located on a large tree-lined street are influenced by this position (Amasyali and El-Gohary, 2018). In particular, the following figures refer to a number of buildings

located in the *Einaudi* area, distinguishing different periods of construction. Figure 7 shows an example of measured and calculated monthly space heating consumption of a residential building built in 1919-45.

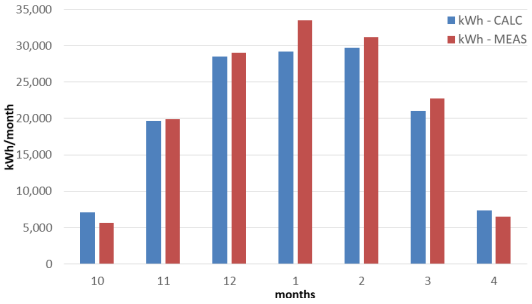

Fig. 7 – Monthly energy consumption for the season 2014-15: building 'E-129', bottom-up model

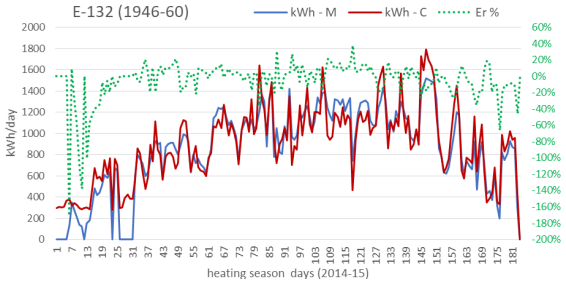

Fig. 8 – Daily consumption and relative error (E_r): building 'E-132', bottom-up model

Figure 8 describes the daily trends for the 2014-15 season of measured and calculated consumption and the daily relative error (E_r). The data refer to the building 'E-132' built in 1946-60. In general, the daily value of E_r varies between ± 20%. Figure 9 shows the cumulative frequency of the 'E-227' building (period 1961-70). It is possible to observe that the model is quite accurate (the greatest inaccuracy occurs in the months of October and April due to the imprecision of measured data at the beginning and the end of the heating season).

In future research, by improving the model with the introduction of other urban parameters (for example, considering the presence of vegetation), it will be possible to optimize the trend of energy consumption (high and low values). Considering the results obtained from the comparison between the *Einaudi* and *Sacchi* neighbourhoods (Fig. 10), it is possible to confirm that the canyon effect is very important in the simulation of energy consumption because it creates a microclimate around buildings by increasing the air temperature and, consequently a lower consumption will occur. Figure 10 shows that when H/ W decreases, the SVF increases and therefore the consumption also increases. Furthermore, the canyon effect and the extra flow are more significant than the solar gains in an urban environment (Mutani et al., 2019).

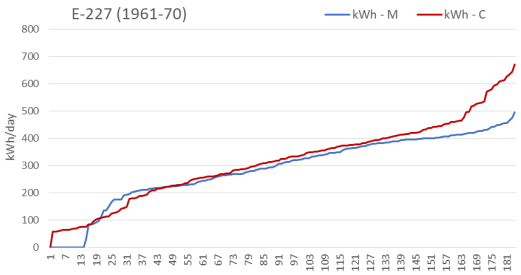

Fig. 9 – Cumulative curves: 'E-227', bottom-up model

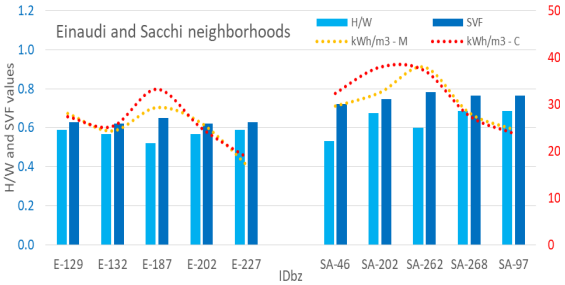

Fig. 10 – Comparison between energy consumption (measured and calculated) and urban parameters for buildings located in *Einaudi* and *Sacchi* neighborhoods

4.2 Bagging Model

With a MAPE of 14.12 % and a R^2 of 0.71, the data-driven model showed good precision on the sample. It was able to reproduce the hourly energy profiles of the buildings with an acceptable degree of error despite the low number of available observations compared to the complexity of the problem. A first comparison with the previous model is given in Figure 11, where the monthly energy demand of building 'E-129' is estimated again. The estimations of the bagging algorithm in this case were slightly more precise, and the tendency was to underestimate the energy consumption, as opposed to the bottom-up model where the errors were mostly on the positive side.

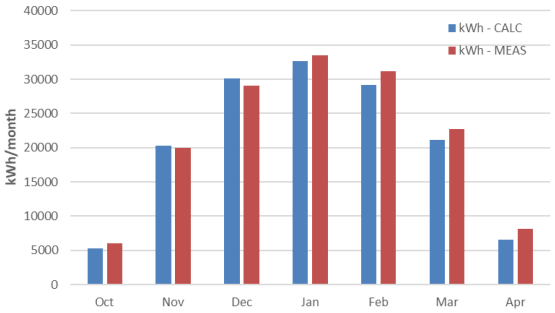

Fig. 11 – Monthly energy consumption for the season 2014-15: building 'E-129', bagging model

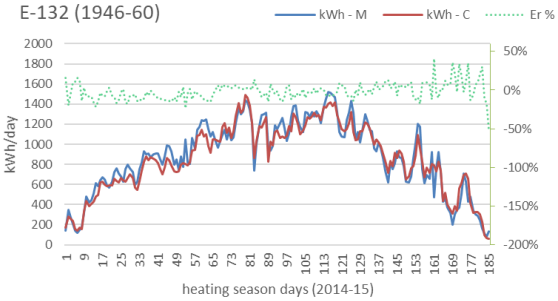

Fig. 12 – Daily consumption and relative error (E_r): building 'E-132', bagging model

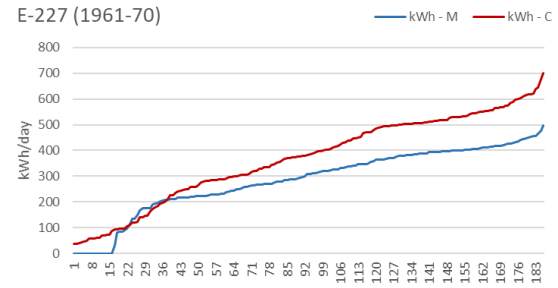

Fig. 13 – Cumulative curves: 'E-227', bagging model

With respect to daily energy demand, Figure 12 shows the performances of the model on building 'E-132'. Again, the error is generally contained within +20% and -20%, which is in line with literature values given the lack of information needed to characterize the human behavior. Both models were therefore able to output a good estimation without notable discrepancies with the real values. Similar to what happened with monthly values, the daily charts show that the two models tend to respectively overestimate and underestimate the real energy consumption.

As previously done with the bottom-up model, Figure 13 finally shows the cumulative frequency of the 'E-227' building. Again, the highest inaccuracy occurred in the months of October and April. While the total error at the end of the heating season was similar for the two models, their short-term behaviours were very different. The bagging algorithm accumulated its error gradually, as opposed to the bottom-up model where the error spiked to its final value mostly during the last month.

Table 2 – Comparison between results of two building energy models

	Bottom-up model				Bagging model			
ID_{bz}	E_r	$\|E_r\|$	Calc.	Meas.	Er	|Er|	Calc.	Meas.
	%		kWh/m³/y		%		kWh/m³/y	
E-129	1	17	27.99	27.30	-11	9	24.89	27.30
E-132	-6	15	24.26	25.23	0	0	25.38	25.23
E-187	-13	17	29.26	33.18	-10	14	28.57	33.18
E-202	-1	19	25.91	24.85	0	13	28.12	24.85
E-227	-7	20	17.07	18.74	19	30	24.36	18.74
S-46	-5	17	29.57	32.28	-6	6	30.48	32.28
S-202	-15	24	32.44	37.87	12	13	40.76	37.87
S-262	2	19	37.87	37.15	-12	16	31.19	37.15
S-268	3	17	28.16	27.52	2	2	28.18	27.52
S-97	4	16	24.54	23.75	16	25	29.65	23.75

4.3 Energy Models Comparison

An overview of the performances of the two models is given in Table 2. Overall, both models showed good performances and their errors were in line with the typical values of the energy performance gap. The precision of the data driven model, however, was less stable, ranging from an absolute error of 30% to less than 1% depending on the building. This behavior is possibly due to the lack of representative buildings of all kinds in the training set, which is a common problem of this approach.

5. Conclusions

Improving the precision of urban-scale energy simulations is an important step to achieve a more efficient use of energy resources. In this work, two simple energy models, which make use of morphological urban-scale parameters in order to take into account the effect of building-to-building interactions, were presented and studied.

The two models were i) a bottom-up engineering approach, ii) a machine learning approach based on the bootstrap aggregating (bagging) algorithm. Both models were able to estimate the hourly consumption of buildings with a low error compared to the expected performance gap that characterize

the problem. The precision of the bagging model, however, was more dependent on the building's characteristics: this behaviour is caused by the lack of representative datapoints in the training set. This reliance on having a good amount of comprehensive data, and the resulting poor generalizability of the model, are the main weaknesses of this approach. On the other hand, the bottom-up model requires longer times and human efforts to produce the output, while also lacking flexibility if one or more building features are missing.

Future work will aim at lessening the weaknesses of both models, for example by smoothing the workflow of the first model and by gathering more data for the second one; and at introducing more morphological parameters as well as properly studying their importance and their impact on the two models.

Nomenclature

A	area
c	specific heat capacity
C	thermal capacity
F	reduction factor
H/W	canyon height-to-distance ratio
ID	identification code
I	solar irradiance
m	mass-related
R	thermal resistance
S/V	surface-to-volume ratio
SVF	sky view factor
t	time
T	temperature
U	thermal transmittance
V	volume
τ	total solar energy transmittance
α	solar radiation absorption coefficient
η	system efficiency
Φ	heat flow rate, thermal power

Subscripts

a	air
B	building
bz	building zone
e	external
E	opaque envelope
G	glass
H	Heating
I	internal heat gains
i	internal
p	opaque
r	radiative (extra flux)
s	surface
sh	shading

References

Amasyali, K., and N. M. El-Gohary. 2018. "A review of data-driven building energy consumption prediction studies." *Renewable and Sustainable Energy Reviews* 81: 1192-1205. doi: 10.1016/j.rser.2017.04.095

Boghetti, R., F. Fantozzi, J. H. Kämpf, and G. Salvadori. 2019. "Understanding the performance gap: a machine learning approach on residential buildings in Turin, Italy." *JPCS* 1343 (1).

Breiman, L. 1996. "Bagging predictors." *Machine learning* 24(2): 123-140. doi: 10.1007/BF00058655.

Caruso, G., F. Fantozzi, F. Leccese. 2013 "Optimal theoretical building form to minimize direct solar irradiation." *Solar Energy* 97: 128-137. doi: 10.1016/j.solener.2013.08.010

IEA. 2019. "Perspectives for the Clean Energy Transition. The Critical Role of Buildings." www.iea.org/publications/reports/PerspectivesfortheCleanEnergyTransition/.

Hedegaard, R. E., M. H. Kristensen, T. H. Pedersen, A. Brun, S. Petersen. 2019. "Bottom-up modelling methodology for urban-scale analysis of residential space heating demand response." *Applied Energy* 242 :181–204. doi: 10.1016/J.APENERGY.2019.03.063

Middela, A., J. Lukasczyk, R. Maciejewski, M. Demuzere, and M. Roth. 2018. "Sky View Factor footprints for urban climate modeling." *Urban Climate* 25: 120-134. doi: 10.1016/j.uclim.2018.05.004

Mutani, G., and V. Todeschi. 2018. "Energy Resilience, Vulnerability and Risk in Urban Spaces." *Journal of Sustainable Development of Energy, Water and Environment Systems* 6(4): 694-709. doi: 10.13044/j.sdewes.d6.0203

Mutani, G., and V. Todeschi. 2019. "An Urban Energy Atlas and Engineering Model for Resilient Cities." *International Journal of Heat and Technology* 37(4): 936-947. doi: 10.18280/ijht.370402

Mutani, G., and V. Todeschi. under revision. "Building Energy Modeling at Neighborhood Scale." *Energy Efficiency*.

Mutani, G., V. Todeschi, G. Grisolia, and L. Lucia. 2019. "Introduction to Constructal Law

Analysis for a Simplified Hourly Energy Balance Model of Residential Buildings at District Scale." *TI-IJES* 6(1): 13–20. doi: 10.18280/ti-ijes.630102

Nageler, P., G. Zahrer, R. Heimrath, T. Mach, F. Mauthner, I. Leusbrock, H. Schranzhofer, and C. Hochenauer. 2017. "Novel validated method for GIS based automated dynamic urban building energy simulations." *Energy* 139: 142-154. doi: 10.1016/j.energy.2017.07.151

Palme, M., L. Inostroza, G. Villacreses, A. Lobato-Cordero, and C. Carrasco. 2017. "From urban climate to energy consumption. Enhancing building performance simulation by including the urban heat island effect." *Energy and Buildings* 145: 107-120. doi: 10.1016/j.enbuild.2017.03.069

Pedregosa et al. 2011. "Scikit-learn: Machine Learning in Python." JMLR 12: 2825-2830.

Perera, A. T. D., S. Coccolo, J. L. Scartezzini, and D. Mauree. 2018. "Quantifying the impact of urban climate by extending the boundaries of urban energy system modeling." *Applied Energy* 222: 847-860. doi: 10.1016/j.apenergy.2018.04.004

Sola, A., C. Corchero, J. Salom, and M. Sanmarti. 2018. "Simulation tools to build urban-scale energy models: A review." *Energies* 11(12): 3269. doi: 10.3390/en11123269

Streicher, K. N., P. Padey, D. Parra, M. C. Bürer, S. Schneider, and M. K. Patel. 2019. "Analysis of space heating demand in the Swiss residential building stock: Element-based bottom-up model of archetype buildings." *Energy and Buildings* 184: 300-322. doi: 10.1016/j.enbuild.2018.12.011

Verbeke, S., and A. Audenaert. 2018. "Thermal inertia in buildings: A review of impacts across climate and building use." *Renewable and Sustainable Energy Reviews* 82: 2300-2318. doi: 10.1016/j.rser.2017.08.083